Catalysis Letters 5 (1990) 143–154

^{129}Xe-NMR STUDY OF COKE DISTRIBUTION IN DEALUMINATED HY ZEOLITES

M.C. BARRAGE, J.L. BONARDET and J. FRAISSARD

Laboratoire de Chimie des Surfaces - U.R.A. CNRS 870, Université Pierre et Marie Curie,
75252 Paris Cédex, France

Received 29 December 1989; Accepted 26 March 1990

NMR, xenon, coke, zeolite, extra-framework aluminium.

Zeolites coking has been studied by ^{129}Xe-NMR technique. The distribution of the coke is heterogeneous on the supercage surface at low cokage level. When coking increases up to 10% the supercages are lined with coke and the residual internal volume consists of narrow channels. Beyond 10% the coke also affects the external surface of the zeolites, with the formation of coke microcavities between the crystallites. This technique has also enabled us to show the role of extra-framework Al in the cracking activity of zeolites.

1. Introduction

The deactivation of zeolites by carbon deposits (coke) is a crucial problem in industrial cracking. Many studies have shown that this deactivation depends on the nature and the structure of the zeolites [1,2]. Thus, the very rapid deactivation of H-mordenite is related to its unidimensional structure, the slightest particle of coke in a channel being enough to make the active sites inaccessible to the reactants. On the other hand, the deactivation of HY and HZSM-5 zeolites, both of which have a three-dimensional lattice, is very different. It is therefore difficult to attribute this deactivation solely to the pore structure [3]. The more rapid deactivation of HY zeolites can be explained by a heterogeneous coke distribution, in agreement with the distribution of sites of different strengths [3]. These coking phenomena have been studied by various techniques, both physical: ^{13}C-NMR [4,5], X-ray diffraction [6], electron microscopy [7], infra-red spectroscopy [8], EPR [9], and chemical: adsorption [2] and extraction by solvent [10]. We thought that ^{129}Xe-NMR could provide additional information. This technique, developed by Fraissard and Ito [11], shows great potential in the study of porous systems, in particular, of zeolites.

2. Experimental conditions

2.1. SAMPLES CHARACTERISTICS

The reference zeolite (HY-R) is obtained by calcining an ultrastable NH_4Y zeolite (LZY 82 from Union Carbide) for 10 hours at 773 K on a stream of air. This HY-R zeolite is already partially dealuminated.

Three HY-R samples were exposed for 5 minutes, 1 and 12 hours to a stream of n-heptane in nitrogen at 723 K. They contain 3, 10.5 and 15% w/w of coke and are denoted HY-3, HY-10.5 and HY-15, respectively.

At the same time, in order to study the effect of dealumination on coke formation and zeolite deactivation, we studied two samples derived from the reference zeolite, the first having been treated with steam at 923 K (HY-S) and the second having been acid washed after steaming to eliminate (wholly or partially?) the extra-lattice aluminium (HY-SW).

All the samples were pretreated under vacuum at 673 K for 12 hours prior to xenon adsorption. The amount of xenon adsorbed, n, is expressed as the number of atoms per gram of anhydrous zeolite.

2.2. ADSORPTION AND ^{129}Xe-NMR

Xenon is adsorbed at 273, 300, 319 and 338 K for the HY-R, HY-3 and HY-10.5 samples and only at ambient temperature for HY-15, HY-S and HY-SW. Adsorption equilibrium is attained after 30 minutes. The ^{129}Xe-NMR spectra are recorded at the same temperatures on a Bruker CXP 100 spectrometer at 24.9 MHz. The chemical shifts, δ, of the adsorbed xenon are measured relative to xenon gas extrapolated to zero pressure.

3. Results and discussion

3.1. ADSORPTION ISOTHERMS

The adsorption isotherms of xenon between 273 and 338 K are shown in fig. 1. The isosteric heats calculated from these isotherms are listed in table 1.

a) Non-coked samples

Whatever the sample and the temperature, the xenon adsorption isotherms are straight lines. At 300 K, the isotherms are about the same. However, the HY-SW sample adsorbs slightly more than HY-R and HY-S (less than 5% more) for a given pressure in the range $0 < P \leqslant 1200$ Torr. (These isotherms are not drawn in fig. 1.)

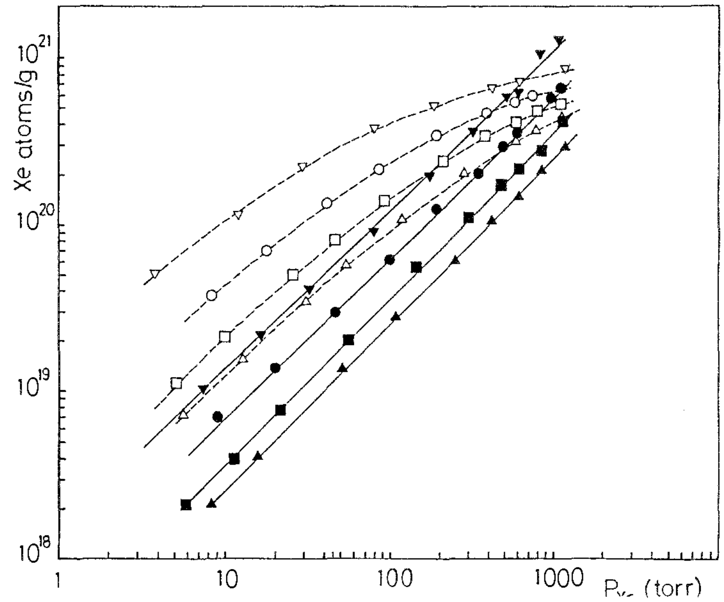

Fig. 1. Xenon adsorption isotherms on HY-R sample at ▼ 273 K, ● 300 K, ■ 319 K, ▲ 338 K. (full lines). Xenon adsorption isotherms on HY-10.5 sample at ▽ 273 K, ○ 300 K, □ 319 K, △ 338 K. (dotted lines).

As for any physical adsorption, the number of Xe atoms adsorbed on HY-R decreases as the equilibrium temperature rises (fig. 1). As is normal, the quantity adsorbed at low pressures increases with the number of charges on the lattice [18]. The very similar isotherms of HY-R, HY-S and HY-SW show that the aluminium concentration is low in all 3 cases. The slightly higher amount adsorbed by HY-SW can be attributed to the increase in the free volume in the cavities, resulting from the partial elimination of the extra-lattice aluminium.

b) Coked samples

At low pressure the xenon adsorption isotherms are straight lines but, the higher the degree of coking, the more they curve at high pressure (fig. 1).

It is also noted that for a given adsorption temperature (300 K) and for a given equilibrium pressure ($P \leqslant 900$ Torr) (fig. 2), the amount of xenon adsorbed at

Table 1
Isosteric adsorption heats (kJ/mol)

n (atoms Xe/g)	HY-R	HY-3	HY-10.5
$1 \cdot 10^{19}$	20.8	29.1	30.4
$5 \cdot 10^{19}$	19.3	25.0	30.4
$1 \cdot 10^{20}$	19.1	24.0	29.1
$3 \cdot 10^{20}$	18.3	21.3	28.3

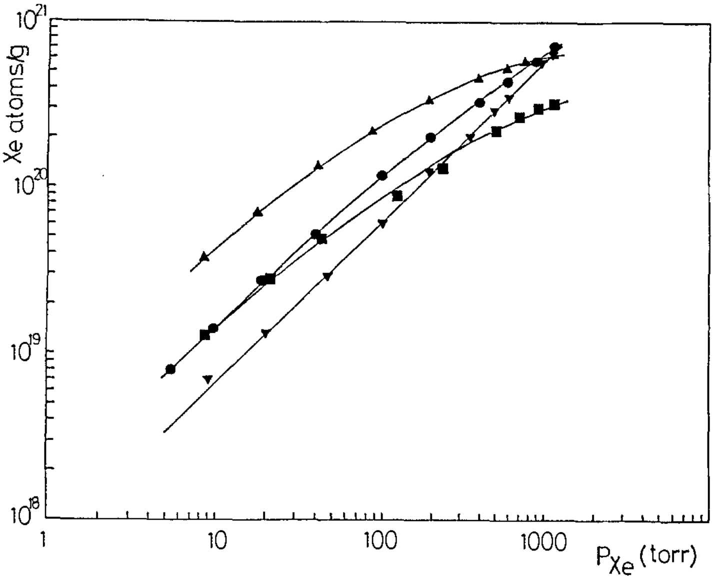

Fig. 2. Xenon adsorption isotherms at 300 K on ▼ HY-R sample, ● HY-3 sample, ▲ HY-10.5 sample, ■ HY-15 sample.

equilibrium increases with the coke concentration as long as it does not exceed 10.5%.

The form and the evolution of the $\ln n = f(\ln P)$ isotherms (fig. 2) can be interpreted as follows:

–At low pressures and for a given temperature the amount adsorbed increases with the coke level up to and including 10.5%. This variation which expresses an increase in the Xe-wall interaction can be explained by the presence of coke lining the supercage walls. This coke can play the part of adsorption centres stronger than the normal zeolite surface. But it can also increase the van der Waals interactions related to the influence of the curvature by decreasing the diameter of these cages [17].

–At high pressure, the decrease in the free volume of the cavities becomes the most important factor. Under these conditions, the amount adsorbed decreases when the coke content increases and it is easy to understand that saturation is reached all the faster when this latter is high.

In the case of HY-15, the reduction of the free volume by the coke more than compensates, even at low pressures, the increase in the Xe-solid interaction.

This interpretation is confirmed by the isosteric adsorption heats (table 1). The isosteric heat is smallest for HY-R and it is practically independent of the extent of coverage. It is also virtually constant for HY-10.5, but 50% higher than in the previous case. This result shows that at this high coke content the surface of the supercages is completely lines with coke. The adsorption heat for sample HY-3 lies between the 2 previous extreme values and it decreases when the Xe concentration increases. This variation corresponds to a heterogeneous distribution of the coke on the supercage surface, the strong adsorption zones, i.e. coked, being occupied preferentially at the onset of adsorption.

3.2. ^{129}Xe-NMR

The high polarisability of the xenon atom makes it very sensitive to its environment. Small variations in the physical interactions with this latter cause marked perturbations of the electron cloud which result in large chemical shifts. Fraissard et al. [11] have shown that the chemical shift of adsorbed xenon is the sum of several terms corresponding to the various perturbations it suffers:

$$\delta = \delta_{\text{ref}} + \delta_{\text{S}} + \delta_{\text{E}} + \delta_{\text{M}} + \delta_{\text{Xe-Xe}}.$$

δ_{ref} represents the chemical shift of gaseous xenon at zero pressure, taken as the reference; therefore $\delta_{\text{ref}} = 0$.
δ_{S} correspond to the chemical shift extrapolated to zero pressure from the asymptote of the curve; it depends on the Xe-wall interaction.
δ_{E} and δ_{M} expresses the contribution of the electric and (possibly) magnetic fields, respectively, created by the compensating cations.
$\delta_{\text{Xe-Xe}}$ corresponds to the chemical shift due to Xe-Xe collisions. This term becomes predominant at high pressure.
The $\delta = f(n)$ curves can be characterized by 3 factors:

–δ_{S} defined above: it depends on the mean free path of xenon, imposed by the zeolite structure, which depends on the dimensions of the cages or channels and on the ease of diffusion of the atoms [16]. It depends also, especially at low temperature, on the Xe-surface interaction [17].

–$\delta_{n \to 0}$ which is the chemical shift extrapolated to zero pressure when the $\delta = f(n)$ curve is not a straight line; like δ_{S}, it depends on the mean free path and on the Xe-surface interaction, but also on the presence of more or less strong adsorption sites [18].

–the slope $\mathrm{d}\delta/\mathrm{d}n$ of the linear section of the curve, which depends on the void volume of the cavities and on the Xe-Xe interactions.
The values of δ_{S} and of the slope are listed in table 2. (The values of $\delta_{n \to 0}$ cannot be determined accurately enough to be given here.)

The NMR spectra of all the samples except HY-15 show a single symmetrical, relatively narrow component which broadens when the coke level increases; the HY-15 spectrum usually has 3 components (fig. 8).
The $\delta = f(n)$ curves are presented in figs. 3–7.

a) Non-coked samples

The $\delta = f(n)$ curves for samples HY-R at 319 and 338 K (fig. 3) are straight lines as for a non-dealuminated HY zeolite, which we have studied elsewhere. For this latter, the δ dependence on n is linear whatever the temperature between 213

Table 2

δ_S (ppm)					slopes of $\delta = f(n)$ curves (ppm/atoms.g^{-1})$\times 10^{20}$			
T (K)	273	300	319	338	273	300	319	338
Non-dealuminated HY		58.0				4.3		
HY-S		59.5				5.6		
HY-SW		63.5				4.7		
HY-R	63.0	59.2	56.5	55.0	5.3	4.9	4.7	4.5
HY-3	78.0	74.0	69.8	64.0	5.1	4.5	4.3	3.6
HY-10.5	76.2	77.5	76.2	79.5	10.7	10.9	10.7	9.9
HY-15		104.0				10.9		

and 300 K [20]. However, at 300 K and especially at 273 K and $\delta = f(n)$ variation of HY-R is similar to that described by Ito and Fraissard [18] for CaY and MgY zeolites and by Gedeon et al. [19] for NiY; that is, in all cases where there are adsorption centres stronger than H^+ or Na^+. We therefore attribute the curvature observed at low xenon concentration to the electric field created by the extra-lattice aluminium atoms, equivalent to more or less complexed Al^{3+} cations.

In the case of HY-S, steaming leads to more dealumination as compared to HY-R; the extra-lattice aluminium concentration therefore increases. It is easy to understand then that the low pressure curvature, expressing the electric effect of cations, would be greater, as is observed experimentally for the HY-S sample (fig. 4).

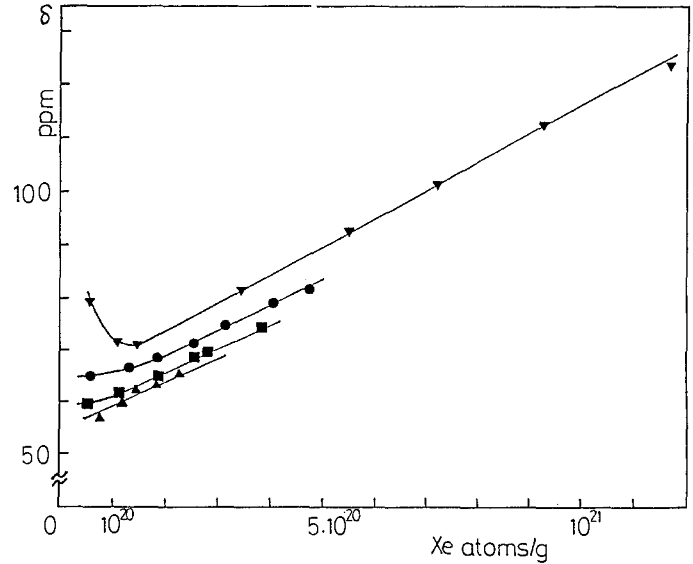

Fig. 3. ^{129}Xe-NMR chemical shifts as a function of sorbed xenon (atoms.g^{-1}) for HY-R sample at ▼ 273 K, ● 300 K, ■ 319 K, ▲ 338 K.

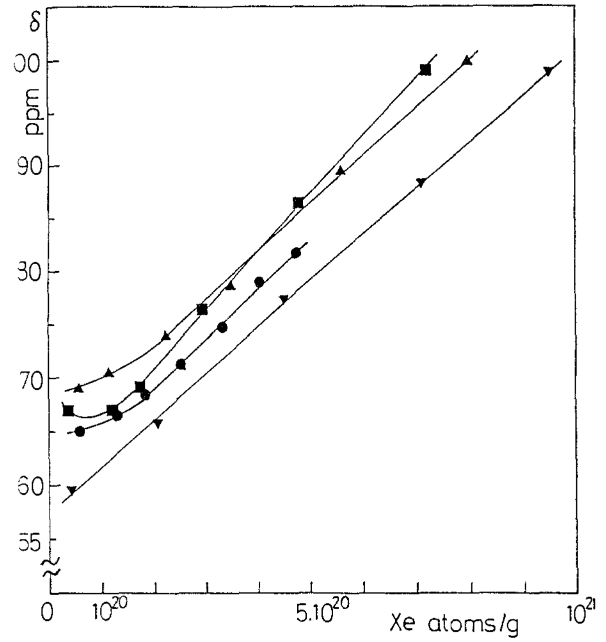

Fig. 4. ^{129}Xe-NMR chemical shifts as a function of sorbed xenon (atoms.g^{-1}) at 300 K for ● HY-R sample, ■ HY-S sample, ▲ HY-SW sample, ▼ non-dealuminated HY sample.

Acid wash leads to partial elimination of the extra-lattice aluminiums and, therefore, to a decrease in their electrical effect; consequently the $\delta = f(n)$ curvature at low concentrations is less for HY-SW (fig. 4).

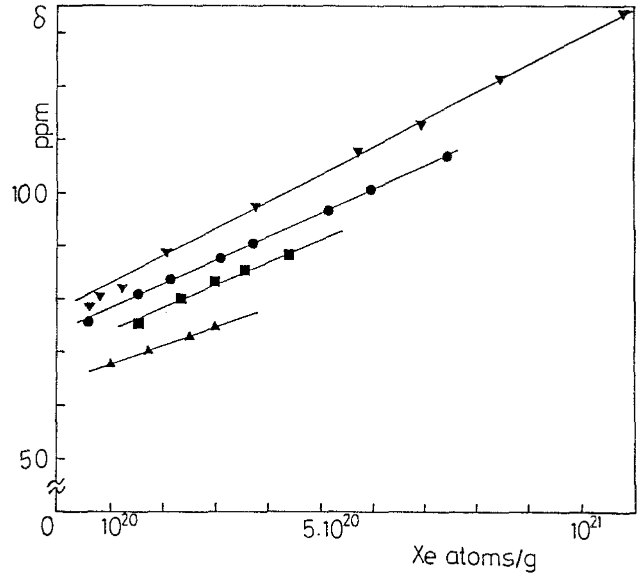

Fig. 5. ^{129}Xe-NMR chemical shifts as a function of sorbed xenon (atoms.g^{-1}) for HY-3 sample at ▼ 273 K, ● 300 K, ■ 319 K, ▲ 338 K.

The variation of the slope $d\delta/dn$ confirms this hypothesis: it is greater for HY-S than for HY-R; dealumination causes a slight decrease in the void volume of the cavities due to the presence of extra-lattice AlO_x groups. The acid wash (HY-SW), by eliminating some of these groups, increases the void volume of the cavities and leads, therefore, to a decrease in $d\delta/dn$. This slope is again slightly higher than that of non-dealuminated HY (table 2) treated under the same experimental conditions, which shows that the extra-lattice AlO_x groups have not been completely eliminated. This result is confirmed by the variation of the ^{27}Al-NMR signal of the extra-lattice Al [20]: steaming leads to the appearance of two signals at 0 and 30 ppm due to hexa and penta (?) coordinated extra-framework aluminium; acid wash removes the 30 ppm signal and reduces the intensity of the 0 ppm signal.

b) Coked samples

For HY-3 (fig 5) and HY-10.5 (fig. 6) the $\delta = f(n)$ variations are linear over the entire concentration range whatever the experimental temperature. As against the presence of a minimum which is more or less pronounced depending on the temperature for HY-R, this linearity shows that the coke is deposited first of all on the extra-lattice aluminiums. At the same time, the HY zeolites lose more than half their activity in heptane cracking when the coke content reaches 3% [1]. We can deduce from these results that the extra-lattice aluminium atoms play a part in the cracking activity of these zeolites.

For HY-10.5, δ_S and the slope $d\delta/dn$ are temperature independent (fig. 6). This result is similar to that obtained for zeolites with narrow channels. It must be assumed therefore that the high coke concentration considerably reduces the mean free path of xenon and that the coke has markedly reduced the diameters of the cages and windows, as is shown in scheme b of fig. 9. The 211 K isotherms show that the amount of xenon adsorbed at saturation is divided by 2.5 compared to the non-coked reference sample. This result is confirmed by the slope $d\delta/dn$ which is 2.4 times that of HY-R [11]. The free volume accessible to the xenon is therefore divided by the same factor; under these conditions the size of the cavities still accessible to the xenon becomes of the same order of magnitude as the size of the xenon atom. Let us consider then the case of rapid exchange between 2 sites characterized by shifts δ_A and δ_V, where δ_A represents the shift of xenon on the internal surface of the cavity and δ_V that of xenon in the volume between 2 collisions. If p_A and p_V are the populations of the 2 sites, then:

$$\delta = p_A\delta_A + p_V\delta_V \quad (p_A + p_V = 1).$$

When the volume becomes small (of the same order of magnitude as the size of the xenon atom), one has:

$$\delta_A \simeq \delta_V \text{ and } \delta = \delta_A = \delta_V.$$

Extrapolated to zero pressure, δ expresses δ_S which is independent of the experimental conditions. This is what is found for this sample.

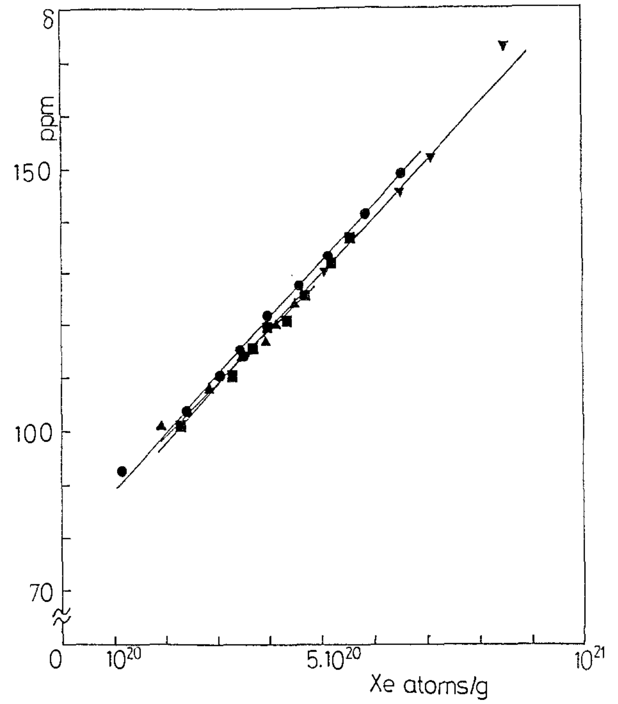

Fig. 6. ^{129}Xe-NMR chemical shifts as a function of sorbed xenon (atoms.g^{-1}) for HY-10.5 sample at ▼ 273 K, ● 300 K, ■ 319 K, ▲ 338 K.

For sample HY-3, δ_S and the slope $d\delta/dn$ depend on the temperature, this being a situation intermediate between the non-coked sample HY-R and the highly coked one HY-10.5 (fig. 5). The slope of HY-3 for each temperature is close to that of the reference sample (table 2), which proves that the volume occupied by the coke is not very great, as expected from its concentration.
The value of δ_S for HY-3, however, is greater than that of HY-R (table 2), which proves that the mean free path of xenon imposed by the structure has decreased. Given that the slope has not changed we can conclude that this decrease is due to the more restricted diffusion of the xenon through the 7.4 Å windows where most of the coke is situated at the beginning of coking. (schema a of fig. 9).

On the other hand, comparison of HY-3 and HY-10.5 at 300 K (fig. 7) reveals that the slope increases very much with the coke level, since this latter then considerably affects the void volume of the cavities. But at the same time δ_S increases much less. This can be explained by the fact that at low coke and xenon concentrations the xenon is preferentially adsorbed on the strongest sites, i.e. coked, as we saw above when the isosteric adsorption heats were calculated.

HY-15 was only studied at 300 K, since each spectrum requires nearly 24 hours accumulation. As we said before, the high pressure spectrum consists of three lines:

–For the broad component the $\delta = f(n)$ variation is linear (fig. 7) and the

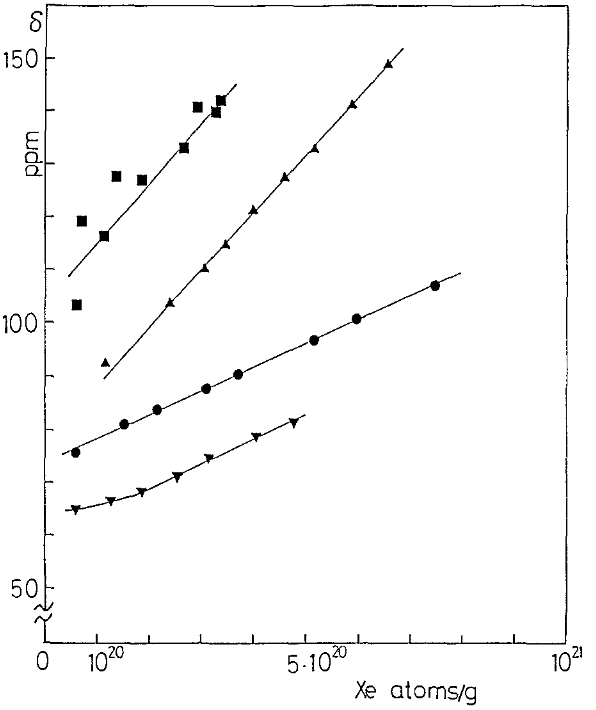

Fig. 7. ^{129}Xe-NMR chemical shifts as a function of sorbed xenon (atoms.g^{-1}) at 300 K for ▼ HY-R sample, ● HY-3 sample, ▲ HY-10.5 sample, ■ HY-15 sample.

slope corresponds to that of HY-10.5. This shows that beyond a coke content of 10.5%, coke mainly affects the external surface of the zeolite. On the other hand δ_S (104 ppm) is much greater than that of the less coked samples: this indicates

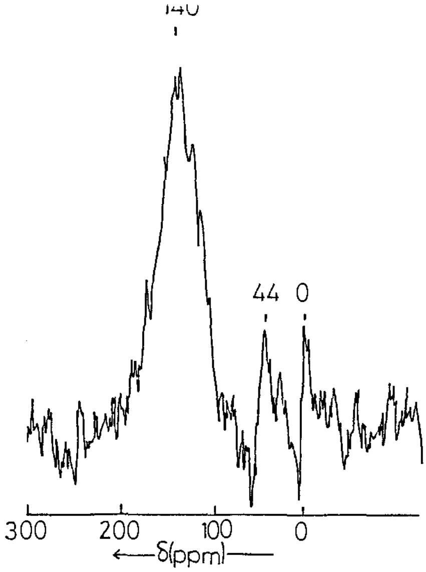

Fig. 8. ^{129}Xe-NMR spectrum of HY-15 sample at 300 K: P_{Xe} = 1200 Torr.

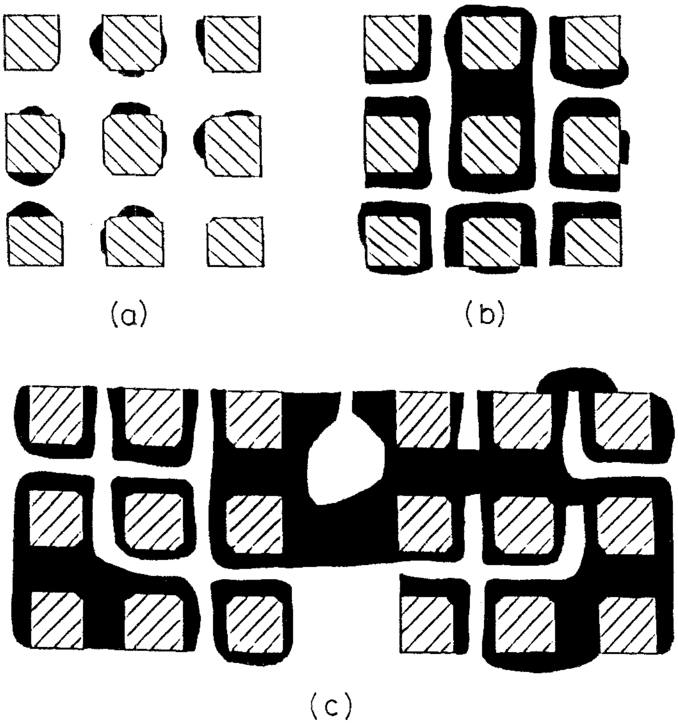

Fig. 9. Schematic representations of coke distribution: scheme a: in the HY-3 sample, scheme b: in the HY-10.5 sample, scheme c: in the HY-15 sample.

that the xenon adsorbed in the residual free volume can only diffuse very slowly from one cavity to another and that the windows are practically blocked (schema c of fig. 9).

–The component at 40–50 ppm is independent of the equilibrium pressure. It can be attributed to xenon adsorbed in the microcavities of coke formed outside the crystallite or between 2 crystallites. A similar signal, even less shifted ($\simeq 10$ ppm) was observed by Ito et al. [12] for a HY zeolite coked to the extent of 33% by propene.

–Finally, the signal observed at relatively high pressure, at about 0 ppm, can be attributed to xenon adsorbed in the coke macropores outside the zeolite or, possibly, to gaseous xenon whose relaxation time has been considerably reduced by the presence of paramagnetic centres due to the external coke.

4. Conclusion

^{129}Xe-NMR is an interesting additional tool for studying zeolite coking. It has enables us to show that the extra-framework Al atoms are among the first coke formation centres, which in return seems to prove that these sites are strongly acidic or near a strong acid site. In this case one can understand the marked deactivation, even at low cokage levels of partially dealuminated HY zeolites.

The evolution of the $\delta = f(n)$ curves shows that at low coke content, xenon diffusion is mainly affected by a narrowing of the windows between supercages. When coking increases, the supercages are then lined with coke, which considerably reduces their diameter. The number of coke-lined supercages increases with the coking. When this reaches about 10% the residual internal volume consists of channels whose diameter is close to that of xenon, which explains why δ hardly varies with the temperature. The existence of several NMR signals, when the coke content is over 10.5%, shows that the coke affects not only the internal volume of the cages but also the external surface of the zeolites, with the formation of coke microcavities between the crystallites.

Acknowledgements

We warmly thank Mr. Magnoux for preparing the samples, Mr. Guisnet for stimulating discussions and Koninklijke/Shell Laboratorium Amsterdam, for financial assistance.

References

[1] P. Magnoux, P. Cartraud, S. Mignard and M. Guisnet, J. Catal. 106 (1987) 235.
[2] P. Magnoux, P. Cartraud, S. Mignard and M. Guisnet, J. Catal. 106 (1987) 242.
[3] M. Guisnet and P. Magnoux, Appl. Catal. 54 (1989) 1.
[4] E.G. Derouane, J.P. Gilson and J.B. Nagy, Zeolites 2 (1982) 42.
[5] S. Maixner, C.Y. Chen, P.J. Grobet, P.A. Jacobs and J. Weitkamp, Stud. Surf. Sci. Catal. 28 (1986) 693.
[6] D.M. Bibby, N.B. Milestone, J.E. Patterson and L.P. Aldridge, J. Catal. 97 (1986) 493.
[7] P. Gallezot, G. Leclercq, M. Guisnet and P. Magnoux, J. Catal. 114 (1988) 100.
[8] D. Eisenbach and G. Gallei, J. Catal. 56 (1979) 377.
[9] P. Dejaifve, A. Auroux, P.C. Gravelle, J.C. Vedrine, Z. Gabelica and E.G. Derouane, J. Catal. 70 (1981) 123.
[10] M. Guisnet, P. Magnoux and C. Canaff, in: R. Setton (ed.), NATO ASI Series C, Vol. 165, *Chemical Reactions in Organic and Inorganic Constrained Systems* (Reidel Publishing Company, Dordrecht, 1985) p. 131.
[11] J. Fraissard and T. Ito, Zeolites 8 (1988) 350.
[12] T. Ito, J.L. Bonardet and J. Fraissard, J.B. Nagy, C. André, Z. Gabelica and E.G. Derouane, Appl. Catal. 43 (1988) L 5-L 11.
[13] J. Demarquay and J. Fraissard, Chem. Phys. Lett. 136, n° 3, 4 (1987) 314.
[14] T. Ito and J. Fraissard, J. Chem. Phys. 76 (1982) 5225.
[15] L.C. de Menorval, T. Ito and J. Fraissard, J. Chem. Soc., Faraday Trans. 1, 78 (1982) 403.
[16] M.A. Springuel-Huet, J. Demarquay, T. Ito and J. Fraissard, *Proc. Int. Symp. on Innovation in Zeolite Materials Science*, Niewpoort, Belgium Sept. 13–17, 1987.
[17] E.G. Derouane and J.B. Nagy, Chem. Phys. Lett. 137, n° 4 (1987) 341.
[18] T. Ito and J. Fraissard, J. Chem. Soc., Faraday Trans. 1, 83 (1987) 451.
[19] A. Gedeon, J.L. Bonardet, T. Ito and J. Fraissard, J. Phys. Chem. 93 (1989) 2563.
[20] Unpublished results.